A novel inline mixer for highly viscous fluid: the proof of concept

Eliane Younes, Yann Moguen, Yves Le Guer, Kamal El Omari, Cathy Castelain, Teodor Burghelea

A novel inline mixer for highly viscous fluid: the proof of concept

Eliane YOUNES[1,2*], Kamal EL OMARI[2], Yann MOGUEN[2], Yves LE GUER[2], Cathy CASTELAIN[1], Teodor BURGHELEA[1]

[1]Université de Nantes, CNRS, Laboratoire de Thermique et Energie de Nantes, UMR 6607, La Chantrerie, Rue Christian Pauc, B.P. 50609, 44306 Nantes Cedex 3, France
[2] Univ. & Pau et Pays Adour/ E2S UPPA, Laboratoire des Sciences pour l'Ingénieur Appliquées à la Mécanique et au Génie Électrique - Fédération IPRA, EA4581, 64000, Pau, France
*(eliane.younes@univ-nantes.fr)

Abstract - The central aim of this paper is to introduce a novel active inline mixer able to efficiently mix highly viscous fluids by laminar chaotic advection. The perturbation of the flow is imposed by three rotating arc-walls in a plane channel. By simple scaling arguments we demonstrate that a good mixing could be obtained corresponding to an optimum value of the Strouhal number that depends solely on the Péclet number and the ratio between angular speed of the walls and axial velocity of the flow. This phenomenological conclusion is corroborated by the results of direct numerical simulations.

Nomenclature

A	area, m^2
C	tracer concentration
d	diffusion length, m
D	mass diffusivity, m^2/s
L	length, m
k	time-averaged velocity ratio
K	maximal velocity ratio
P	pressure, Pa
Pe	Péclet number
R	radius, m
Re	Reynolds number
St	Strouhal number
t	time, s
T	period of rotation, s
U	inlet velocity, $\mathrm{m/s}$
V	velocity, $\mathrm{m/s}$
W	width, m
y	transversal coordinate, m

Greek symbols

Δ	depth of protrusion, m
μ	dynamic viscosity, $\mathrm{Pa.s}$
ξ	length ratio
ρ	density, $\mathrm{Kg/m^3}$
σ	mixing indicator
τ	time unit, s
Ω	rotational speed, $\mathrm{rad/s}$

Index and exponent

c	cell
m	mixing
r	residence
t	tangentiel
0	amplitude
$*$	non-dimensional parameter
$-$	time-averaged
min	minimum
max	maximum
$1, 2, 3$	numbering index

1. Introduction

Mixing of pasty materials in the absence of inertial contributions (i.e. at low Reynolds numbers Re) is primordial to many industrial applications related to food processing, cosmetics, biotechnology and oil field industry. For highly viscous fluids the natural mixing mechanism via molecular diffusion is highly insufficient. Enhancement and reduction of the timescale of mixing could be achieved by generating inertial turbulence in the flow. However, for highly viscous fluids achieving high Re translates into additional energetic costs and risks of degradation of the texture of the final product. Hence, the increase of Re becomes problematic. Yet, a

solution exists which consists of triggering laminar chaotic advection to promote mixing. In a two-dimensional steady flow, laminar chaotic advection may be triggered by a time dependent forcing of the flow [1].

Given the two available options of batch [1, 2] and open flow inline mixers [3], we chose the latter for several reasons: high production rates and a reduction of operating time by eliminating filling and pump-out cycles. Inline mixers may be either passive [4, 5] or active [6, 7, 8]. In this study, we focus on a two-dimensional active inline mixing concept.

Traditional inline mixers currently used in industries remain to this day not fully optimised, essentially because the mixing is carried out throughout the entire length of the flow channel by using moving objects [9, 10]. When the mixing length becomes larger than required, several drawbacks appear. For instance, degradation of the product could be triggered by over-mixing, not to mention the increased final product price to compensate the additional input energy during the over-mixing.

Given the above mentioned reasons, we propose in the current study a novel active inline mixer with three rotating arc walls aimed to locally mix highly viscous fluids. The paper is organised as follows. The concept of the rotating arc walls mixer is introduced in Sec. 2.1. Simple scaling arguments for the concept of the rotating arc-walls mixer are presented in Sec. 2.2. Preliminary numerical simulations which fully corroborate the theoretical arguments are detailed in Sec. 2.3. The paper closes with a summary of the main conclusions and several perspectives, Sec. 3.

2. The rotating arc-walls mixer

2.1. Design of the rotating arc-walls mixer

A sketch of the rotating arc-walls mixer (RAW mixer) is illustrated in Fig. 1. The RAW mixer is composed of a plane channel of width W and length $L = 5W$, with three circular cylinders of equal radii $R = \dfrac{W}{2}$ having their axis of rotation perpendicular to the plane of the channel. The cylinders penetrate into the channel with a depth of protrusion $\Delta = \dfrac{W}{6}$.

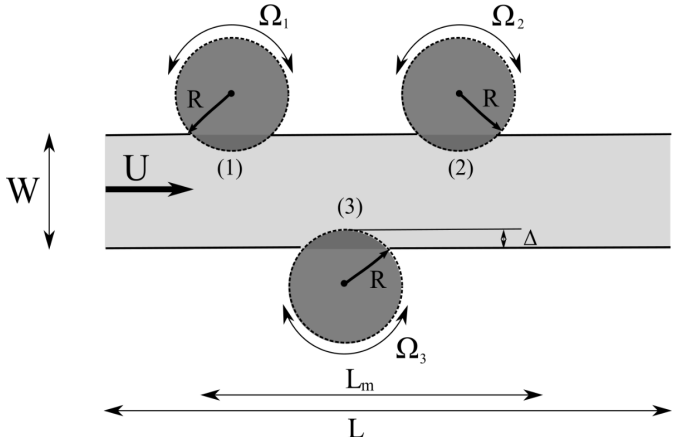

Figure 1 : *Schematic illustration of the rotating arc-walls mixer.*

Chaotic mixing is developed by modulating the rotational speed of the cylinders in relation

with the mean input velocity U. The three cylinders oscillates at the same period T and amplitude Ω_0. The upper ones are synchronized $\Omega_{1,2}(t) = \Omega_0 \sin\left(\frac{2\pi}{T}t\right)$ while the rotation of the bottom one is phase shifted by an angle of π, $\Omega_3(t) = -\Omega_0 \sin\left(\frac{2\pi}{T}t\right)$.

2.2. Scaling arguments to predict the mixing condition

The mixing problem is governed by the following non-dimensional numbers:

1. The Péclet number defined as $Pe = \frac{UW}{D}$ where U the incoming mean flow speed and D the molecular diffusion coefficient.
2. The Strouhal number defined as $St = \frac{W}{TU}$ where T is the period of rotation of the arc-walls.
3. The velocity ratio $k = \frac{\overline{V_t}}{U}$ represents the ratio of the time-averaged tangential speed of the rotating arc-walls $\overline{V_t}$ to the mean inlet velocity U.
4. The non-dimensional mixing length introduced as $\xi = \frac{L_m}{W}$ where L_m is the length of the mixing zone, see Fig. 1.

The interface between two fluids is initially located at mid-width of the channel. We assume that to insure an efficient mixing the displacement of a fluid particle initially located near a wall should exceed half of the channel width $\frac{W}{2}$ during half a period $\frac{T}{2}$. This condition translates into a first inequality:

$$k \geq St \tag{1}$$

The idea behind the RAW mixer concept is that the cylinders will generate chaotic Lagrangian structures in the flow. The chaotic advection will stretch, fold and split fluid elements down to the scale:

$$d = \frac{W}{2^n} \tag{2}$$

Here d is the characteristic diffusion length and $n-1$ is the number of stretching and folding cycles undergone by the fluid elements. Then, the corresponding characteristic time for diffusion after $n-1$ cycles is:

$$t_m = \frac{d^2}{D} = \frac{W^2}{4^n D} \tag{3}$$

A phenomenological condition for the mixing of two fluid elements to be efficient is that the characteristic mixing time t_m should be smaller or equal to the characteristic residence time t_r in the mixing zone.

$$t_m \leq t_r \tag{4}$$

The characteristic residence time may be estimated as $t_r = \frac{L_m}{U}$. Then, the mixing condition (4) becomes:

$$n \geq \frac{1}{ln(4)} \ln\left(\frac{Pe}{\xi}\right) \tag{5}$$

At this point, we find it useful to write the characteristic residence time t_r as: $t_r = nT + \delta t$ where $0 \leq \delta t \leq T$. With the mixing conditions (1) and (5) we obtain:

$$k \geq \frac{1}{\xi ln(4)} \ln\left(\frac{Pe}{\xi}\right) \tag{6}$$

We define the tangential speed of a cylinder as $\overline{V_t} = \overline{\Omega} R$ where $\overline{\Omega}$ is the angular speed of a rotating cylinder averaged over the characteristic residence time of a fluid particle in the mixing zone:

$$\overline{\Omega} = \frac{1}{t_r} \int_0^{t_r} \Omega_0 \left|\sin\left(\frac{2\pi t}{T}\right)\right| \mathrm{d}t \tag{7}$$

From the inequality (6) and Eq. (7), we obtain the following mixing condition:

$$\boxed{K \geq \frac{\pi St}{\ln(4)} \frac{\ln\left(\frac{Pe}{\xi}\right)}{2n + sin^2(\pi \xi St)}} \tag{8}$$

Here K is defined by $K = \dfrac{\Omega_0 R}{U}$.

Fig. 2(a) displays the theoretical mixing surface defined by Eq. 8 for $n = 1$ and $\xi \approx 2$. For any given Pe, the space (St, K) may be divided in two regions by a curve $K = K(St)$ which has a local minimum, Fig. 2(b). The region of the space (St, K) above this curve corresponds to good mixing whereas the region below corresponds to poor mixing.

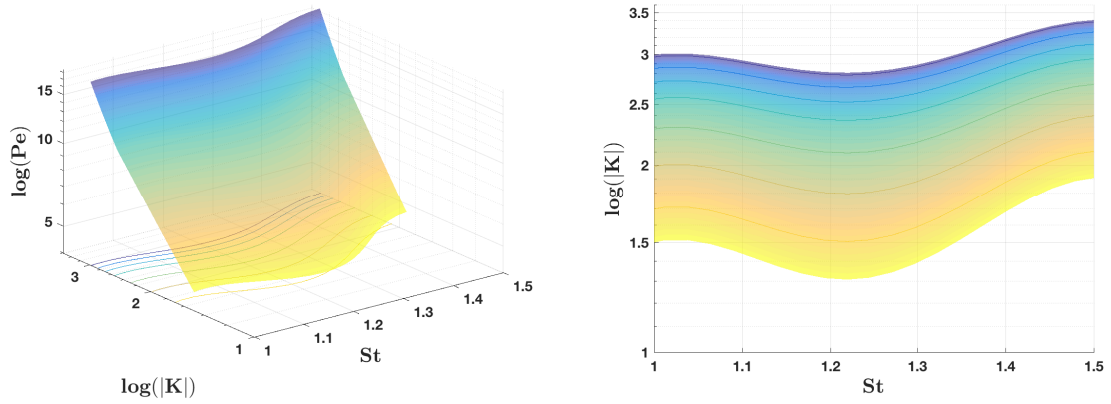

(a) (b)

Figure 2 : *(a) Mixing efficiency surface based on correlation (8). (b) Projection of the mixing surface onto ($St - K$) plane. Different colours/contours refers to different Pe.*

To achieve better mixing, it is evident that the Strouhal number St should be increased by simply decreasing the period of rotation T (faster forcing). However, from the analytical solution given in (8), there exists an optimal Strouhal number St, beyond which the increase of St results in a decrease of fluid displacement and thus in a loss of the mixture quality.

It is important to mention that several minima exist corresponding to different ranges of Strouhal number meaning that for each range of St the rotational speed of the cylinders should be adapted to the mean inlet velocity of the flow.

2.3. Numerical simulations

To validate the simple physical arguments presented in Sec. 2.2., two-dimensional direct numerical simulations were performed using a CFD code developed in-house already validated in a number of previous studies [11, 12, 13]. The non-dimensional continuity (9), momentum (10) and advection-diffusion (11) equations were solved for a time-dependent laminar incompressible newtonian fluid flow.

$$\nabla \cdot \mathbf{V}^* = 0 \tag{9}$$

$$\frac{\partial \mathbf{V}^*}{\partial t^*} + (\mathbf{V}^* \cdot \nabla)\mathbf{V}^* = -\nabla P + \frac{1}{Re}\nabla \cdot \left((\nabla \mathbf{V}^*) + (\nabla \mathbf{V}^*)^{\mathrm{T}}\right) \tag{10}$$

$$\frac{\partial C^*}{\partial t^*} + \nabla(\mathbf{V}^* \cdot C^*) = \frac{1}{St}\nabla^2 C^* \tag{11}$$

Here $C^* = \dfrac{C - C_{min}}{C_{max} - C_{min}}$ ($C_{min} = 0$ and $C_{max} = 1$), $\mathbf{V}^* = \dfrac{\mathbf{V}}{U}$ and $t^* = \dfrac{t}{\tau}$ are respectively the dimensionless concentration, velocity and time. τ is the unit time $\tau = \dfrac{W}{U}$.

2.3.1. Numerical method and mixing indicator

The equations (9, 10, 11) are solved by the means of an unstructured finite volume method using an unstructured finite grid of 24 000 cells (tetrahedral, hexahedral) generated by the open-source code Gmsh [14]. The grid independence of the numerical results was tested by comparing simulations performed with various grid refinements.

The concentration field is initially distributed as:

$$\begin{cases} C^* = 0 & for \quad 0 \leq y^* \leq \frac{1}{2} \\ C^* = 1 & for \quad \frac{1}{2} \leq y^* \leq 1 \end{cases} \tag{12}$$

Here $y^* = \dfrac{y}{W}$ is the non-dimensional coordinate in a direction transversal to the mean flow.

One classical measure for the degree of homogeneity of the mixture is the standard deviation of the concentration C defined as:

$$\sigma = \sqrt{\frac{1}{\sum_c A_c} \sum_c A_c (C_c^* - C_{\mathrm{m}}^*)^2} \tag{13}$$

Here C_c is the concentration in the mesh cell, A_c is the area of the mesh cell and C_m^* in the mean concentration in the entire region calculated as:

$$C_{\mathrm{m}}^* = \frac{1}{\sum_c A_c} \sum A_c C_c^* \tag{14}$$

The standard deviation of the scalar field calculated in a zone of width $0.285\ W$ located downstream of the three cylinders and averaged on the last five periods of rotation.

2.3.2. Fluid properties and boundary conditions

Two identical Newtonian fluids with a density $\rho = 10^3\ kg.m^{-3}$, a dynamic viscosity $\mu = 1\ Pa.s$ and a molecular diffusion $D = 10^{-9}\ m^2/s$ are considered as working fluids.

A Poiseuille velocity profile is imposed at the inlet and no-slip boundary condition is prescribed at the solid walls.

The rotational speed of the cylinders 1 and 2 on the top wall varies in time according to:

$$V^*_{t_{1,2}}(t^*) = K \sin(2\pi St\, t^*) \tag{15}$$

The cylinder 3 on the bottom wall is phase shifted by π with respect to the oscillation of the first two cylinders:

$$V^*_{t_3}(t^*) = -K \sin(2\pi St\, t^*) \tag{16}$$

2.3.3. Numerical results

We show in Fig. 3(a) the temporal evolution of the scalar field along the RAW mixer. These results refer to $St = 1$, $K = 40$, $Re = 1$ and $Pe = 10^6$. It is clear that the mixing is progressively achieved as the fluid traverses the channel and as the time passes.
As time progresses one notes the formation of Lagrangian coherent structures in the flow separated by a hyperbolic points essential for the mixing of two fluids by laminar chaotic advection.

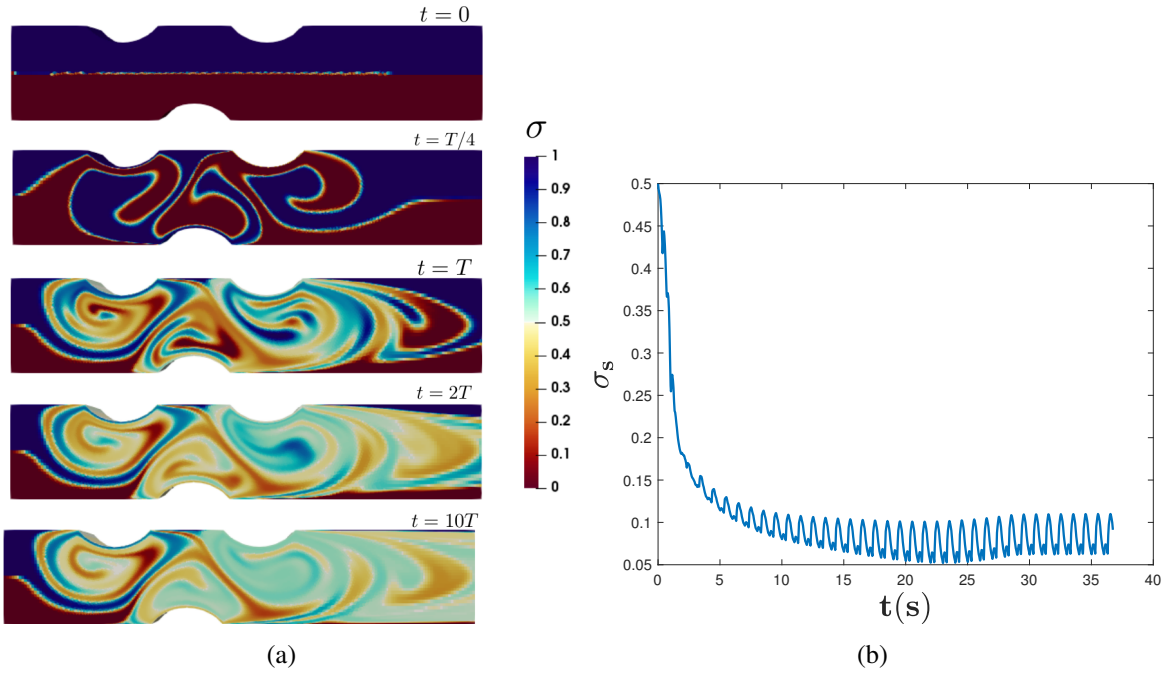

(a) (b)

Figure 3 : *(a) Temporal evolution of the scalar field along the RAW mixer. (b) Temporal evolution of the standard deviation σ of the scalar field.*

The mixing efficiency defined as the standard deviation σ of the scalar field C is presented in Fig. 3(b). It decreases from 0.5 at $t = 0$ when the two fluids are separated by a straight interface to a value close to zero after a finite time when the two fluids are perfectly mixed.

The simulations are repeated for several St and K at a fixed $Re = 1$ and $Pe = 10^6$. The mixing efficiency results of 96 interpolated numerical simulations are summarised in Fig. 4.

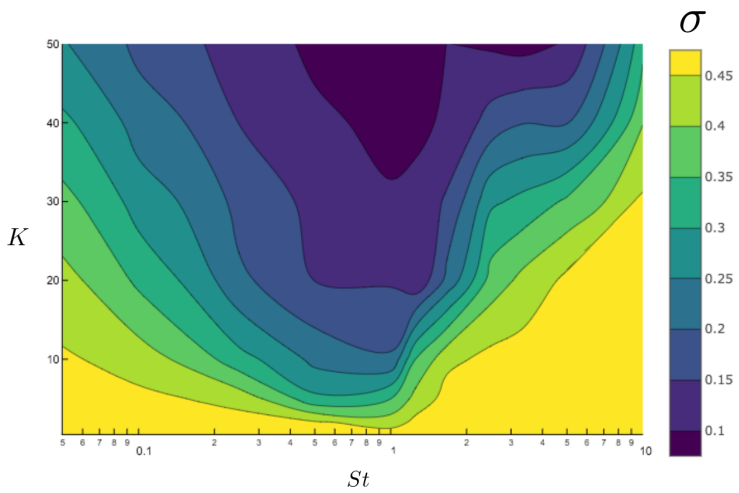

Figure 4 : *Variation of the standard deviation of the scalar field C according to the Strouhal number and the velocity ratio at constant $Re = 1$.*

The mixing efficiency map presented in Fig. 4 indicates the existence of an optimal St as theoretically predicted and an increase of the mixing efficiency when K is increased.

3. Conclusions, outlook

The objective of this study was to efficiently mix highly viscous fluids at minimal energetic costs. This was achieved by implementing a novel type of inline mixer that uses the laminar chaotic advection as a mechanism to mix such viscous fluids by generating Lagrangian coherent structures.Three rotating arc-walls induce an unsteady perturbation of the flow essential to achieve efficient mixing in a two dimensional system.

Simple scaling arguments prove the feasibility of the mixing strategy. We derived analytically an optimum mixing condition in terms of angular speed of the walls, Strouhal number and Péclet number.

To reinforce the theoretical predictions, numerical simulations were performed. The numerical results confirmed the existence of an optimum Strouhal number and thus the validity of our simplified physical model.

This study helped us to understand the physics underlying the transport process and highlighted the role of the different parameters involved. The next step is to study experimentally the mixing efficiency of the RAW mixer. This novel inline mixer will be later used to homogenise the temperature in different industriel processes.

References

[1] H. Aref, The development of chaotic advection. Physics of Fluids, 14-4 (2002) 1315-1325.

[2] D. Patel, F. Ein-Mozaffari, M. Mehrvar, Characterization of the continuous-flow mixing of non-Newtonian fluids using the ratio of residence time to batch mixing time, Chemical Engineering Research and Design, 91-7 (2013) 1223-1234.

[3] H. A. Kusch, J. M. Ottino, Experiments on mixing in continuous chaotic flows, Journal of Fluid Mechanics, 236 (1992) 319-348.

[4] M. Khosravi Parsa, F. Hormozi, D. Jafari, Mixing enhancement in a passive micromixer with convergent-divergent sinusoidal microchannels and different ratio of amplitude to wave length, Computers and fluids, 105 (2014) 82-90.

[5] O. Baskan, H. Rajaei, M. Speetjens, F. M., H. J. H.Clercx, Scalar transport in inline mixers with spatially periodic flows, Physics of Fluids, 29-1 (2017) 013601.

[6] M. H. Oddy, J. G. Santiago, J. C. Mikkelsen, Electrokinetic Instability Micromixing, Analytical Chemistry, 73-24 (2001) 5822-5832.

[7] L. H. Lu, , S. K. Ryu, C. Liu, , A magnetic microstirrer and array for microfluidic mixing, Journal of microelectromechanical systems, 11-5 (2002) 462-469.

[8] T. J. Ober, D. Foresti, J. A. Lewis, Active mixing of complex fluids at the microscale, Proceedings of the National Academy of Sciences, 112-40 (2015) 12293-12298.

[9] T. A. Kingston, T. J. Heindel, Granular mixing optimization and the influence of operating conditions in a double screw mixer, Powder Technology, 266 (2014) 144-155.

[10] D. R. Lester, M. Rudman, G. Metcalfe, Low Reynolds number scalar transport enhancement in viscous and non-Newtonian fluids, International Journal of Heat and Mass Transfer, 52- 3-4 (2009) 655-664.

[11] K. El Omari, Y. Le Guer, Laminar mixing and heat transfer for constant heat flux boundary condition, Heat and Mass Transfer, 48-8 (2012) 1285-296.

[12] K. El Omari, Y. Le Guer. Alternate rotating walls for thermal chaotic mixing. International, Journal of Heat and Mass Transfer 53-1 (2010) 123-134.

[13] K. El Omari, Y. Le Guer, Thermal chaotic mixing of power-law fluids in a mixer with alternately rotating walls, Journal of Non-Newtonian Fluid Mechanics, 165-11 (2010) 641-651.

[14] C. Geuzaine, J. Remacle, Gmsh: A 3-d finite element mesh generator with built-in pre- and post-processing facilities, International Journal for Numerical Methods in Engineering, 79-11 (2009) 1309-1331.

Acknowledgements

We acknowledge the Agence Nationale de la Recherche (ANR) for the financial support via project NaiMYS (ANR-16-CE06-0003).